Experimental Agriculture (2022), vol. 58, e41, 1–13
doi:10.1017/S0014479722000308

CrossMark

CAMBRIDGE UNIVERSITY PRESS

RESEARCH ARTICLE

Predicting protein content of silage maize using remotely sensed multispectral imagery and proximal leaf sensing

Nikrooz Bagheri*[,1], Maryam Rahimi Jahangirlou[2] and Mehryar Jaberi Aghdam[3]

[1]Agricultural Engineering Research Institute, Agricultural Research, Education and Extension Organization (AREEO), Karaj, Iran, [2]Department of Agronomy and Plant Breeding Sciences, College of Aburaihan, University of Tehran, Tehran, Iran and [3]Department of Agronomy, Varamin-Pishva Branch, Islamic Azad University, Varamin, Iran
*Corresponding Author. Email: n.bagheri@areeo.ac.ir

(Received 13 February 2022; revised 02 July 2022; accepted 19 July 2022)

Abstract

Timely estimation of silage maize protein provides an effective decision to adapt optimized strategies for nitrogen fertilizer management and also harvesting time for farmers. So, this research aimed to investigate whether using vegetative indices (VIs) derived from UAV remotely sensed multispectral (with 520–900 nm wavelengths) imagery and also Soil Plant Analysis Development (SPAD) greenness index can be used to detect the leaf protein concentration (LPC) of silage maize, as a function of various nitrogen rates (0, 50, 100, and 150% of recommended dosage). Results of principal component analysis (PCA) suggested that LPC was highly correlated with leaf greenness index in all developmental stages. In addition, LPC was highly correlated with most of the VIs investigated. A PCA clustering showed the meaningful pattern of N rates. Higher LPC values, VIs, and greenness index were more concentrated in the higher nitrogen (N100% and N150%) sectors. Nitrogen Reflectance Index (NRI) was identified as the most important VIs to monitor and predict LPC in the silage maize field, showing a strong polynomial relationship with LPC in both eight-leaf collar (V8) ($R^2 = 0.81$, $p \leq 0.01$) and tasseling (VT) ($R^2 = 0.98$, $p \leq 0.001$) stages. In addition, among VIs, the Normalized Difference Vegetation Index (NDVI) demonstrated a significant linear regression relationship with LPC ($R^2 = 0.80$, $p \leq 0.01$) in the VT. Findings suggested the high potential of VIs extracted by UAV-taken multispectral imagery and also SPAD proximal sensing to help farmers rapidly diagnose LPC in silage maize, in line with the objectives of precision farming.

Keywords: Nitrogen; Remote sensing; Precision agriculture; Protein; Unmanned Aerial Vehicle (UAV)

Introduction

The maize harvested for silage is one of the most valuable forages for ruminant livestock in the world. Protein content is an important nutritional index for feed crops and is relevant in terms of its overall concentration (Rahimi Jahangirlou *et al.*, 2022). Maize silage contains about 5–10% protein concentration on a dry weight basis (Klopfenstein *et al.*, 2013).

Earlier estimation of nitrogen (N) and protein concentration of silage maize provides an effective decision to adapt optimized strategies for N fertilizer management and also harvesting time (Zhao *et al.*, 2019). The advance of the maturity of maize reduces the crude protein content, neutral detergent fiber (NDF), and acid detergent fiber (ADF) and increases in vitro true digestibility (Darby and Lauer, 2002; Mandić *et al.*, 2018).

Currently, two main types of nondestructive detection methods are used for predicting the protein content of crop organs: (i) crop growth modeling and (ii) remote sensing inversion. In the crop growth modeling method, weather, soil, cultivar, and field management parameters as inputs are being used for predicting protein content in the models such as Agricultural Production Systems SIMulator (APSIM) and Crop Environment Resource Synthesis (CERES) (Chen *et al.*, 2020). Using physiological models is often a time-consuming process and requires a relatively large number of inputs. Remote sensing, as an indirect method, relies on using inversion of vegetation N concentration by canopy spectral reflectance data and calculating various vegetation indices (VIs) based on regression models (Chen *et al.*, 2020; Bagheri *et al.*, 2012). Briefly, the electromagnetic radiation that runs into the leaf surface can be reflected, scattered, absorbed, and transmitted at wavelengths that depend on the biochemical and physical characteristics of the leaf (i.e., sugars, proteins, lignin, and cellulose) (Galieni *et al.*, 2020). Using remotely sensed VIs may offer faster pathways to track crops nutritional traits compared with processed-based models (Chen *et al.*, 2020; Wang and Wei, 2013).

Another promising approach for the rapid and periodic assessment of crop N status and predicting protein in plants is using proximal optical sensors. Proximal optical sensors are positioned either in contact with or close to the crop. Chlorophyll meters are the most important group of optical sensors studied for crop N management (Padilla *et al.*, 2018a). It is reported by recent researches that measuring with all types of chlorophyll meters including SPAD-502 meter, the at LEAF+ sensor, Chlorophyll Content Index (CCI) measured with the MC-100 Chlorophyll Concentration Meter, and the Multiplex's chlorophyll indices of Simple Fluorescence Ratio (SFR), either under red (SFR_R) or green (SFR_G), can be as accurate estimators of leaf N status and chlorophyll content in plants (Padilla *et al.*, 2018b).

Some research has been performed to forecast protein content of various crops using remote sensing data based on the theory that canopy reflectance could predict parameters related to crop growth vigor during the growth season, which, in turn, can be used to estimate the protein content (Chen *et al.*, 2020). Li-Hong *et al.* (2007) found a strong relationship between the leaf N accumulation and Green Ratio Vegetation Index (GRVI) of each wheat cultivar using power relationships ($R^2 = 0.7779$ for 'Huaimai 18' and $R^2 = 0.7871$ for 'Xuzhou 26'). These reports indicated the high accuracy of VIs based on green spectral radiance to predict protein content in winter wheat (Li-Hong *et al.*, 2007). Zhao *et al.* (2019) found a strong correlation coefficient between Sentinel-2A VIs and N parameters at wheat anthesis stage, which provides the potential for the estimation of the wheat protein content through spectral VIs.

As a means of rapid, nondestructive, and large-area simultaneous monitoring, satellite and aerial remote sensing technology have been proved to be useful for the inversion of various physiological and biochemical parameters of crops (Haboudane *et al.*, 2004; Zhao *et al.*, 2019). In addition, high-resolution aerial remote sensing systems could be an accurate alternative to traditional plant testing for the diagnosis of crop N and nutritional status (Bagheri, 2016; Bagheri *et al.*, 2013). However, more research has to perform to assess the accuracy of remote and proximal sensing systems to estimate the nutritional aspects of crop plants in diverse environments. So, the objective of the present research was to (i) assess VIs derived from UAV-based multispectral imagery and Soil Plant Analysis Development (SPAD) greenness index to predict silage maize protein before fully ripens and (ii) develop guidelines to help farmers make effective decisions to adapt optimized strategies for N fertilizer management and timely harvest of maize in semi-arid conditions of Iran.

Materials and Methods

Study area and field experiments

Field experiments were performed on a research farm with an area of 850 m^2 in Varamin city (35.80°N, 51.40°E) (Figure S1). This region has a semiarid climate with relatively cold winters and hot summers. Annual precipitation in Varamin is less than 200 mm, concentrated in late autumn and winter.

Irrigated summer maize in this region is typically cultivated after winter cereals, However, in some areas (due to the benefit of autumn rainfall and the reduction of the impact of the extreme temperature on maize growth), autumn cultivation is also carried out. In this experiment, autumn silage maize (sown on 6 September 2020) was tested. Before cultivation, soil sampling was conducted from the depth of 0–30 cm of soil. The samples were tested for total N using the Kjeldahl method, for available phosphorus (P) and potassium (K) by the Olsen and flame photometer procedures, respectively, and also pH and electrical conductivity (EC). The soil is characterized as clay-loam, and details of soil properties in 0–30 cm soil depth were as follows: total N, 1.1%; available P, 10.4 $mg.L^{-1}$; available K, 410 $mg.L^{-1}$; EC, 3.65 dSm^{-1}; pH, 7.69.

In early October, experimental plots (7.00 m length × 5.20 m width) were designated at the farm. Each plot included 8 rows. The experimental design was randomized complete block design (RCBD) with four replicates (Figure S2). The variable factor was N fertilizer in four rates including 0, 50, 100, and 150% of the recommended dosage according to the soil test. Urea was used as the N source and top dressed in equal proportions when plants were typically on eight leaf collar (V8) and tasseling (VT) growth stages, applied along with irrigation water. An early maturity maize cultivar 450 (Gazda MTC) was used and planted in recommended depth (5 cm) and density (67 000 plant ha^{-1}). An irrigation regime by maize phenological events was specified to create typical nonstressed growing conditions. Furrow irrigation was used for irrigation. The closed-end furrows were constructed with a ditcher. Parshall flume (open channel flow metering device) was used in each irrigation event to determine the irrigation amount and to ensure irrigation uniformity in the experimental units.

Ground sampling

One week after N fertilization at V8 and VT growth stages, ground sampling was performed to measure plant height (H), total fresh weight (TFW), and total dry weight (TDW) of aboveground organs. Ten marked plants were randomly harvested from each sampling region to represent the homogenous plot. After measuring their height, plants were separated into leaves and stems (containing ears only for the R1 stage). All the samples were then oven dried at 70 °C for about 48 h until constant weight. The dried maize organs were weighed for measuring TFW and TDW, then ground, and stored in plastic bags for chemical analysis. Leaf protein concentration (LPC) was determined from 0.20 g of dried samples with the micro-Keldjahl method (Guebel *et al.,* 1991).

In addition, simultaneously with each sampling time, the SPAD chlorophyll index was measured using a 502-chlorophyll measuring device (Minolta Corp., Osaka, Japan) after calibration of the device. Three readings were taken from the base, middle, and top of each leaf, and the averaged data were used for processing. SPAD chlorophyll data were recorded when plants were typically on two (V2), four (V4), eight (V8) leaf collars and also tasseling (VT) and silking (R1) stages of maize growth.

Acquiring and processing aerial imagery

Aerial multispectral UAV imaging was performed in two stages (V8 and VT growth stages), simultaneous with each fertilization and ground sampling. To reduce the effects of solar zenith angle (SZA) and sun azimuth angle (SAA) variations on reflectance, the images were captured between 11:00 am and 12:00 local time. All flights were carried out in stable ambient light conditions with a fixed flight speed and route planning during the entire season from a height of 100 m above the ground. ADC-Micro multispectral camera (Tetracam, Inc, Gainesville, FL, USA) with 520–900 nm wavelengths in green (520–600 nm), red (630–690 nm), and near-infrared (760–900 nm) channels were used to collect aerial multispectral imagery with the rotary-wings UAV developed by Bagheri (2016). After capturing and extracting images, aerial images were processed using ENVI 5.4 software. The radiometric correction was performed using a white Teflon calibration plate. Preprocessing of images included changing the image format from DCM to TIFF, creating false-color images, and radiometric correction of images done using PixelWrench2 software. Vegetation indices including Normalized Difference Vegetation Index (NDVI), Nitrogen Reflectance Index (NRI), Modified Triangular Vegetation Index2 (MTVI2), Chlorophyll Index (CI), Green Model (GM), Modified Chlorophyll Absorption Ratio Index (MCARI), and Anthocyanin Reflectance Index (ARI) were associated with plant chlorophyll and N content and were calculated using equations shown in Table 1.

Table 1. Vegetation indices equations reflecting the chlorophyll and nitrogen status of maize plants

Index	Equation	Reference
ARI	$\left(\frac{1}{G} - \frac{1}{R}\right)$	Gitelson *et al.* (2009)
CI	$\frac{\mathrm{NIR}}{G} - 1$	Smith *et al.* (2008)
GM	(NIR-*G*)-1	Devadas *et al.* (2009)
MTVI2	$\frac{1.5 \times [1.2(NIR-G)-2.5(R-G)]}{\sqrt{-0.5+(2NIR+1)^2-\left(6NIR-5\sqrt{R}\right)}}$	Bagheri *et al.* (2013)
MCARI1	$1.2 \times [1.2(R800 - R550) - 2.5(R670 - R550)]$	Nguy-Robertson (2013)
MCARI2	$\frac{1.5 \times [2.5(R800-R670)-1.3(R800-R550)]}{\sqrt{(2R800+1)^2-(6R800-5\sqrt{R670})-0.5}}$	Nguy-Robertson (2013)
NDVI	$\frac{\mathrm{NIR}-R}{\mathrm{NIR}+R}$	Reum and Zhang (2007)
NRI	$\frac{G-R}{G+R}$	Corti *et al.* (2019)

ARI, Anthocyanin Reflectance Index; CI, Chlorophyll Index; GM, Green Model; MTVI2, Modified Triangular Vegetation Index 2; MCARI1, Modified Chlorophyll Absorption in Reflectance Index 1; MCARI2, Modified Chlorophyll Absorption in Reflectance Index 2; NDVI, Normalized Difference Vegetation Index; NRI, Nitrogen Reflectance Index.

Data analysis

To investigate the effect of N fertilizer rates on crop growth attributes (H, TDW, and TFW), LPC and VIs, their values in each sampling and imaging stage, were analyzed using RCBD procedures in SAS, v.9.4 software. Tukey's statistic was used to test differences ($p \leq 0.05$) among means. Principal component analysis (PCA) was carried out using Minitab, v.19 to understand the relationships among variables and N fertilizer rates. Classification and regression tree (CART) analysis and relative importance chart were used to uncover relationships and interactions between crop growth traits of maize crop and VIs using Minitab, v.19. Various regression models were fitted to VIs and LPC to understand if there was a significant relationship between them and create meaningful equations for LPC prediction.

Results and Discussion

Effects of N fertilizer on growth attributes, SPAD greenness index, and LPC

The results of the mean comparison of ground sampling variables in the V8 and the VT growth stages are shown in Figure 1. Results indicated that there was a significant effect of N on LPC in both V8 and VT growth stages (Figure 1a). According to the figure, the amount of LPC increased with increasing the amount of the N fertilizer dosage. The highest LPC value in the V8 (7.37%DM) and the VT (7.34%DM) belonged to the highest N rate (N150%) (Figure 1a). Higher LPC with higher N rates was relevant to the results reported by Cao *et al.* (2018) who suggested that normally there is a positive correlation between the N application and the protein content. This is because N element utilization stimulates the activity of panel enzymes involved in protein biosynthesis (Gous *et al.*, 2015). In addition, Rahimi Jahangirlou *et al.* (2022) reported that according

https://doi.org/10.1017/S0014479722000308 Published online by Cambridge University Press

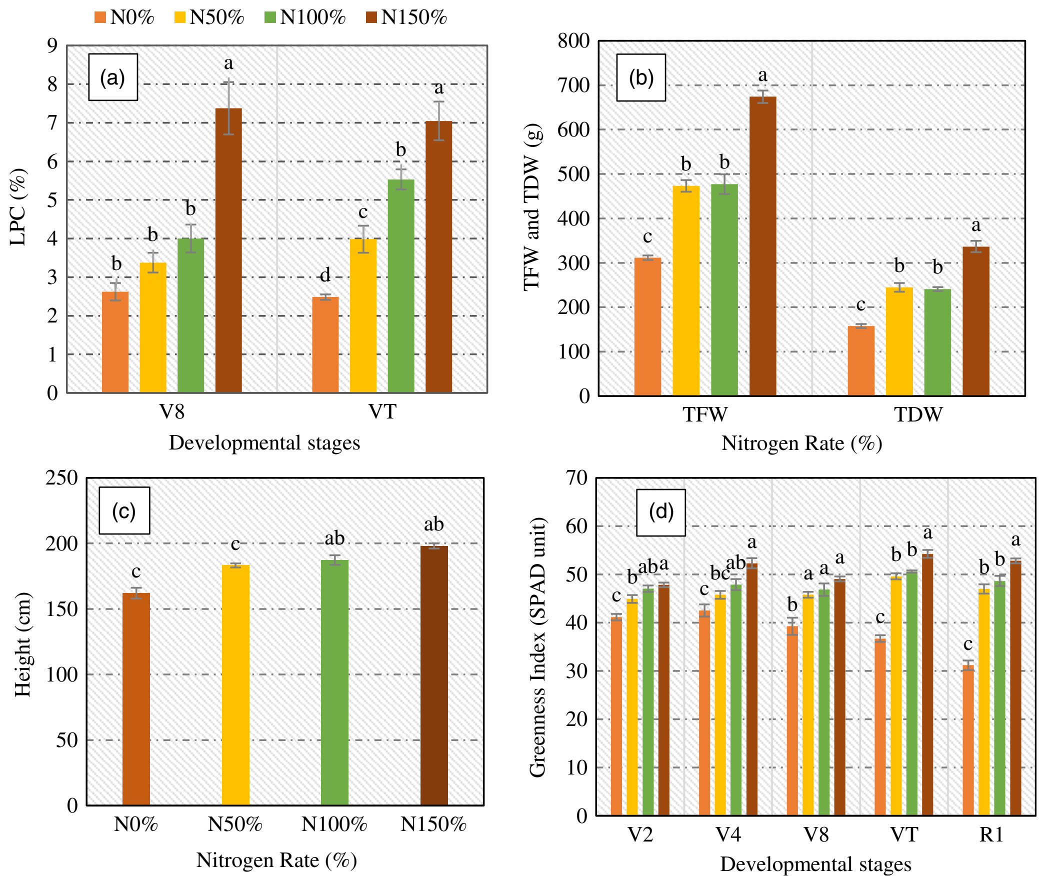

Figure 1. Means of leaf protein content (LPC) in the eight leaf collar (V8) and tasseling (VT) growth stages (a), total fresh weight (TFW) and total dry weight (TDW) (b) and plant height (c) in VT growth stage, and leaf greenness index in various developmental stages of silage maize (d) in response to different nitrogen fertilizer dosages. Means labeled with the same letter do not differ significantly at $p \leq 0.05$ based on Tukey's test. Vertical bars represent the standard error of the mean. SPAD, Soil Plant Analysis Development.

to the decision tree regression, among different genetics and management practices, N fertilizer rate was the most important factor in determining the protein concentration of maize grain.

The results showed that there was a significant effect of N on morphophysiological variables including TFW and TDW (Figure 1b), and also plant height (Figure 1c). The highest N rate (N150%) increased TFW (640.00 g) and TDW (336.73 g) to the maximum extent ($p < 0.001$) (Figure 1b). Compared to the plots without N fertilizer (N0), average height was higher in N contained plots, i.e., N150% (198 cm), N100% (187.25 cm), and N50% (183.25 cm), without significant difference ($p < 0.001$) (Figure 1c).

The higher biomass of aerial organs and also plant height with the higher N rates were expected because the N application improves the N uptake and accumulation by leaves, and it is strongly correlated with higher chlorophyll content, higher chloroplast activities, and higher photosynthetic rate and biomass accumulation (Rahimi Jahangirlou *et al.*, 2021b). Higher N regimes expectedly increase dry matter accumulation in maize by enhancing leaf area and chlorophyll content, absorption of solar radiation, and biomass partitioning to individual organs (Rahimi Jahangirlou *et al.*, 2021b).

https://doi.org/10.1017/S0014479722000308 Published online by Cambridge University Press

According to the results, there was a significant effect of N on the leaf greenness index of maize plants in all developmental stages of silage maize including V2, V4, V8, VT, and R1 (Figure 1d). Leaf greenness index was higher in V2 (47.80 and 47.05 SPAD unit) and V4 (52.30 and 47.80 SPAD unit) growth stages in plots containing N100% and N150%, respectively, without significant difference ($p < 0.001$). Moreover, the SPAD leaf greenness index in V8 was higher in N contained plots (N150%= 49.05, N100%=46.83, and N50%=45.77 SPAD units), without significant difference ($p < 0.001$). The highest N rate (N150%) had the highest SPAD leaf greenness index in the VT (54.22 SPAD unit) and R1 (52.80 SPAD unit) stages, compared to the other N rates ($p < 0.001$). In general, the SPAD leaf greenness index was higher with N150% than with the other N rates (Figure 1d). Generally, there is a close relationship between SPAD readings and leaf N and protein content per leaf area because N application increases chloroplast in the leaves (Xiong *et al*., 2015). Indeed, the diurnal variation in SPAD readings is a function of species and N supplementation (Xiong *et al*., 2015). Results also suggested that the highest values of all studied variables were obtained at the highest N rate (N150%). Maize during vegetative growth can accumulate luxury N over what is required for biomass accumulation (Nasielski *et al*., 2019). This is a survival strategy in the plant because during post-silking, N uptake is restricted and this luxury N may mitigate N stress by acting as a reservoir that buffers biomass yield and maintains plant function (Nasielski *et al*., 2019). The application of a higher N dosage in this research was adopted to assess the accuracy of VIs to detect high N concentrations in a maize canopy. Otherwise, utilization of higher N rates, excess to the soil requirements and plant consumption, is forbidden due to nutritional and environmental pollution.

Correlations between N fertilizer rates, LPC, and VIs

The PCA results showed that the first two principal components (PCs) accounted for 73.2% of the total variance (Figure 2).

The loading plot (Figure 2a) illustrates the eigenvectors for 26 variables related to maize plants attributes (H, TFW, TDW, LPC), greenness index, and VIs (NDVI, NRI, MTVI2, ARI, MCARI1, MCARI2, CI, GM) in two separate times of sampling and imaging (V8 and VT growth stages). In the loading plot, LPCa and LPCb were designated as target variables and accordingly one cluster of highly correlated variables with them was recognized. In this cluster, LPCa and LPCb were highly correlated with all characteristics obtained from ground sampling including TFW and TDW, H, all related to the VT stage. For example, the correlation between LPCa and TDW was 0.84 and the correlation between LPCb and SPAD5 was 0.82. The high correlation between variables belonging to ground sampling is in line with earlier studies that provided the theories based on physiological relationships on the significant effect of N fertilizer on all growth and quality variables, namely protein content (Rahimi Jahangirlou *et al*., 2021a,b).

In addition, the SPAD leaf greenness index in all stages including V2 (SPAD1), V4 (SPAD2), V8 (SPAD3), and VT (SPAD4) and R1 (SPAD5) exhibited a high correlation with LPCa and LPCb. The high correlation between reflectance indices whether aerial or proximal is expected and reported in a previous study by Lin *et al*. (2010), who mentioned RSI (the SPAD ratio of the first and third fully expanded leaf) and RDSI (the SPAD relative positional difference index between the first and third fully expanded leaf) as SPAD meter-based indices were relevant for estimating foliar N and protein status in rice plant.

Considering Figure 2a, all VIs except MCARI and ARI were placed in the same cluster and indicated a high correlation with LPCa and LPCb. For instance, the correlation between LPCa and NRIa was 0.71 and the correlation between LPCa and NDVIa was 0.78. In addition, the correlation between NRIb with LPCa and LPCb was 0.74 and 0.88, respectively. Similarly, it was reported by Zhao *et al*. (2019) that in winter wheat, all VIs derived from the canopy spectral reflectance at the green and red bands in their experiment were significantly correlated to the final grain protein content. They suggested that the spectral reflectance of LandSat TM channel 5 derived

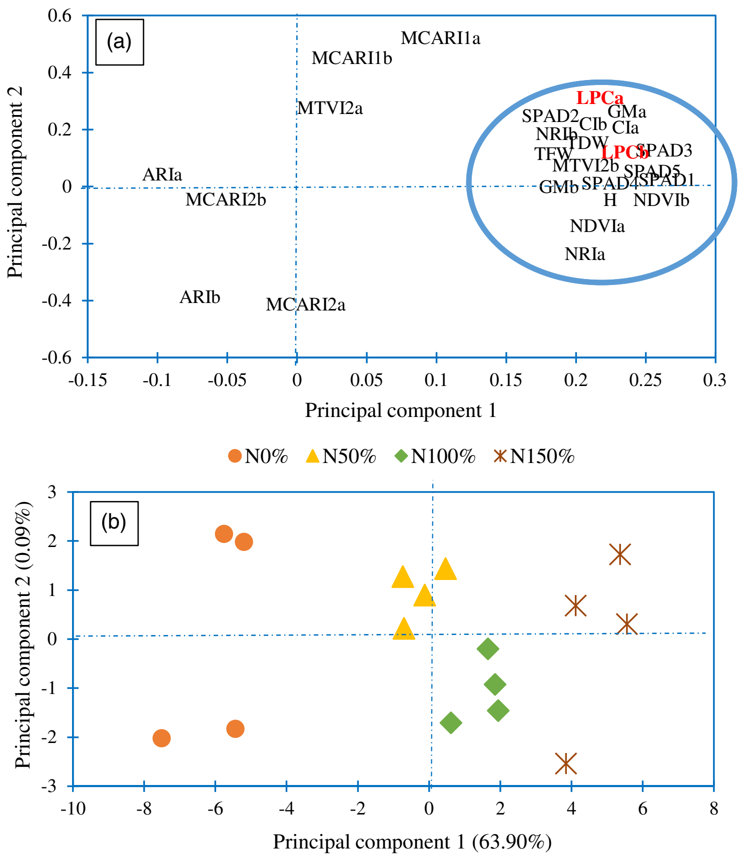

Figure 2. Plots of principal component 1 versus principal component 2 based on measured silage maize variables and vegetation indices: the loading plot (a) shows the eigenvector of each variable, (b) shows the means, grouped by nitrogen fertilizer rates. Abbreviations; H, plant height; TFW, total aboveground fresh weight; TDW, total aboveground dry weight; LPC, leaf protein concentration; NDVI, Normalized Difference Vegetation Index; NRI, Nitrogen Reflectance Index; MTVI2, Modified Triangular Vegetation Index 2; ARI, Anthocyanin Reflectance Index; MCARI1, Modified Chlorophyll Absorption in Reflectance Index 1; MCARI2, Modified Chlorophyll Absorption in Reflectance Index 2; CI, Chlorophyll Index; GM, Green Model; a, V8 stage; b, VT stage; SPAD, Soil Plant Analysis Development; 1, 2, 3, 4, and 5 represent two, four, and eight leaf collar, and tasseling and silking stages of maize growth, respectively.

from canopy spectra or image data at the grain filling period was all significantly correlated to grain protein content ($R^2 = 0.31$ and 0.37, respectively). Pettersson and Eckersten (2007) reported that it was possible, for specific barley cultivars, to make predictions of malting barley grain protein at harvest, from VIs. The index they used was Transformed Chlorophyll in Absorption Index (TCARI) and showed a high correlation with barley grain protein according to the adjusted R^2 of 0.78. In addition, it was suggested by the earlier research that it is possible to explain variations of both grain yield and grain protein content in malting barley using canopy reflectance data from early stem elongation (Pettersson and Eckersten, 2007). Pettersson *et al.* (2006) used TCARI and suggested that this index was the most important control variable and VIs for predicting grain protein. Results of other studies also showed that the VIs like NRI could be used to estimate the within-field variation of yield potential and plant parameters in silage maize (Diker and Bausch, 2003); however, they did not assess the possible relationships among VIs and any quality computes of silage maize like protein. But López-Calderón *et al.* (2020) used 13 VIs to estimate the N content of silage maize, which can also be referred to as the protein content. Their overall

https://doi.org/10.1017/S0014479722000308 Published online by Cambridge University Press

analysis showed five of the 13 indices as the most important, and among them, TCARI was found to be most important for the estimation of N content in forage maize ($R^2 = 0.76$).

The score plot means are shown in Figure 2b. There are four N rates, each one in 4 replicates, providing a combination of 16 samples. The data points presented in the score plot coincide with the direction of changes in variables in the loading plot. A recognized cluster containing the variables correlated with LPCa and LPCb more concentrated in the high N (N100% and N150%) sectors shows the meaningful effect of higher N rates on protein concentration, SPAD greenness index, and most VIs. The score plot results are consistent with the results of the analysis of variance and show the effect of N fertilizer on all measured variables. While few indices (MCARI and ARI) were concentrated in N50%, clusters contained LPCa and LPCb and most of the VIs and growth characteristics were pulled toward N100% and N150%. This is in line with the theory that VIs captured by UAVs are sensitive enough to the greenness degree for responding to the different amounts of N fertilizer (Caturegli *et al.,* 2016). It is reported that UAV imagery in turfgrasses field can adequately assess the N status of different crops and their spatial variability within a species, and proximity-sensed NDVI was highly correlated with data acquired from UAV with r values ranging from 0.83 (Zm) to 0.97 (Cdxt) (Caturegli *et al.,* 2016). Similar results were obtained by other researchers who used UAV-derived multispectral imagery to predict leaf N and protein content in corn (Jaberi-Aghdam *et al.,* 2020) sugarcane (Shendryk *et al.,* 2020), and maize (Xu *et al.*, 2021) using different VIs and wavelet features. Shendryk *et al.,* (2020) used both UAV LiDAR and multispectral imaging for fine-scale prediction of biomass and leaf N content in sugarcane and found that predictive performance peaked early in the season, at 100–142 days after the previous harvest (DAH), and declined closer to the harvest date. At peak performance (i.e., 142 DAH), the multispectral model performed slightly better ($R^2 = 0.57$) than the LiDAR model ($R^2 = 0.25$) with both outperforming the NDVI benchmark ($R^2 = 0.34$). These results could demonstrate the potential of UAV-based multispectral imagery in predicting the N and protein status of crop plants and informing farmers about deficiency or additional fertilization on the farm (Shendryk *et al.,* 2020). Under optimum and super-optimum conditions of irrigation and N fertilization, healthy plants look green because they absorb red bands and reflect the green band of the light spectrum (Hatfield *et al.,* 2008).

To determine the contribution of variables on the leaf protein, a regression tree was fitted for LPCa (Figure 3a) and LPCb (Figure 4a) against all traits and indices. For LPCa, this tree explained a large part of the variation ($R^2 = 79.9\%$, $p \leq 0.001$). The optimum regression tree had one split and two terminal nodes (Figure 3a).

The first split in the tree suggested that the N rate was the most important factor in determining LPCa. This split produced two groups of data: one was N0, N50%, and N100% with an average protein concentration of 3.33% DM, and the other was N150% with an average protein concentration of 7.37% DM (Figure 3a). The chart of the relative importance of LPCa (Figure 3b) includes 14 variables with positive importance, providing information about how many variables to control or monitor for predicting LPCa. Results show that the most important predictor variables were NRIb, SPAD5, TFW, TDW, CIa, SPAD4, N, and MTVI2a. The variables including NDVIa, GMa, SPAD2, H, and NRIa were about 79, 78, 75, 75, and 75% as important as NRIb. Polynomial regression (Figure 3c), as the best model fitted, describes that there is a positive and significant relationship between LPCa and NRIb ($R^2 = 0.81$; $p \leq 0.01$).

For LPCb (Figure 4a), the regression tree explained a large part of the variation ($R^2 = 73.2\%$, $p \leq 0.01$), as well. The optimum regression tree had one split and two terminal nodes, as well. The first split in the tree suggested that the NRIb was the most important factor in determining LPCb. This split produced two groups of data: one was NRIb less than 0.998 with an average protein concentration of 3.02% DM, and the other was NRIb more than 0.998 with an average protein concentration of 6.11% DM (Figure 4a).

The chart of the relative importance of LPCb (Figure 4b) includes 15 variables with positive importance for predicting LPCb. The most important predictor variables were NRIb and NDVIa

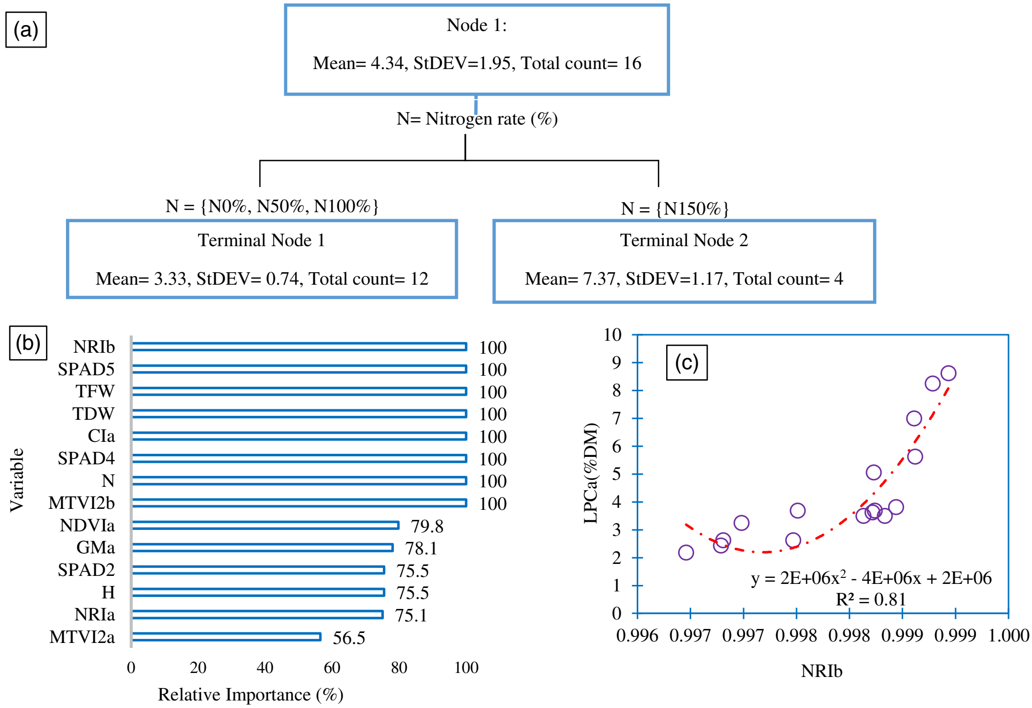

Figure 3. Regression tree predicting leaf protein concentration in V8 stage (LPCa) from variables obtained from ground sampling and UAV aerial multispectral imaging ($R^2 = 79.9\%$, $p \leq 0.001$) (a); chart of the relative importance of variables predicting LPCa of silage maize (b) and the best-fitted model (polynomial regression) between LPCa and Nitrogen Reflectance Index in VT stage (NRIb) (c). Other abbreviations: SPAD, Soil Plant Analysis Development; SPAD5, SPAD in R1; TFW, total fresh weight; TDW, total dry weight; CIa, Chlorophyll Index in V8; SPAD4, SPAD in VT; N, nitrogen fertilizer; MTVI2b, Modified Triangular Vegetation Index 2 in VT; NDVIa, Normalized Difference Vegetation Index in V8; GMa; Green Model in V8; SPAD2, SPAD in V4; H, plant height; NRIa, Nitrogen Reflectance Index in V8; MTVI2a, Modified Triangular Vegetation Index 1 in V8; StDEV, standard deviation. The 'node' is the main classification which represents the entire sample and may get split further into other nodes. 'Terminal node' is the mean of the observations in that node. 'Total count' is the number of observations in each terminal node.

(Figure 4b). The variables including N, SPAD1, and MTVI2b were about 99.6, 99.5, and 95.9% as important as NRIb and NDVIa.

Polynomial regression and linear regression were the best models fitted for NRIb ($R^2 = 0.98$; $p \leq 0.001$, Figure 4c) and NDVIa ($R^2 = 0.80$; $p \leq 0.\ 01$, Figure 4d), respectively, both describe that there is a strong and positive relationship between LPCb, NRIb, and NDVIa. According to the results obtained by the regression tree, the N fertilizer stage was the most important predictor of LPC values in the first stage (V8), while NRI values were the most important predictor of LPC in the tasseling growth stage (VT).

Two potential reasons can be considered for the predominance of a categorical variable such as the N rate in the early stages over the VIs: (1) In early growth, when the canopy is not yet completely closed, compared to the flowering period when there is a peak of greenness and plant biomass, different N levels is a more important factor for classifying the field into two groups of high and low LPC. Consequently, the field showed very heterogeneous patches of crop development in various N levels, (2) due to the effect of bare soil and its noise on images in the early stages, N displayed a greater relationship with protein than the VIs during V8 growth stage. However, according to what the relative importance chart suggested, NRI in both growth stages (V8 and VT) was the most important VIs to control or monitor LPC in the field. In addition, NDVI in the VT

https://doi.org/10.1017/S0014479722000308 Published online by Cambridge University Press

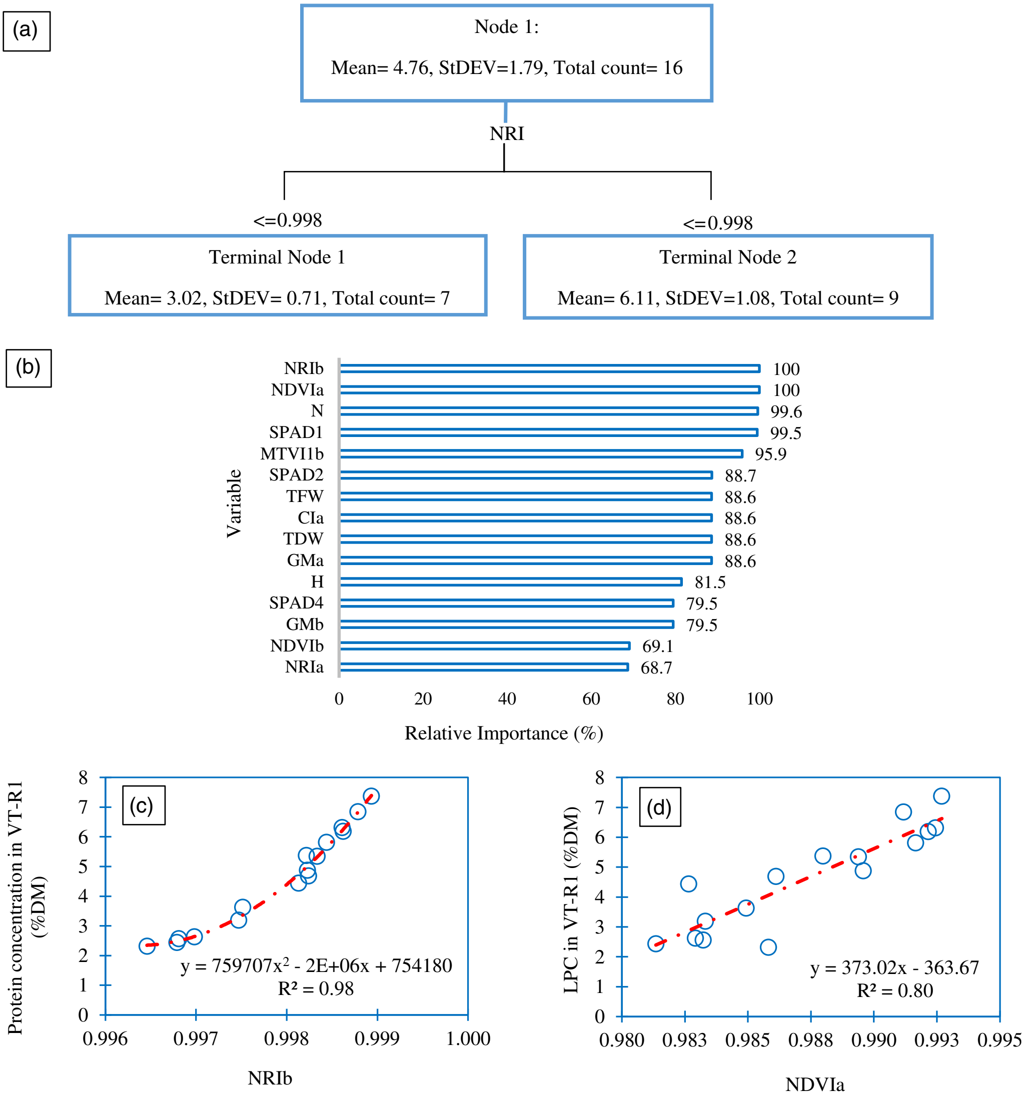

Figure 4. Regression tree predicting leaf protein concentration in VT stage (LPCb) from variables obtained from ground sampling and UAV aerial multispectral imaging ($R^2 = 73.2\%$, $p \leq 0.001$) (a); chart of the relative importance of variables predicting LPCb of silage maize (b) and the best-fitted model (polynomial regression) between LPCb and Nitrogen Reflectance Index in VT stage (NRIb) (c) and Normalized Difference Vegetation Index in V8 (NDVIa) (d). Other abbreviations: N, nitrogen fertilizer; SPAD, Soil Plant Analysis Development; SPAD1, SPAD in V2; MTVI2b, Modified Triangular Vegetation Index 1 in VT; SPAD2, SPAD in V4; TFW, total fresh weight; CIa, Chlorophyll Index in V8; TDW, total dry weight; GMa; Green Model in V8; H, plant height; SPAD4, SPAD in VT; GMb; Green Model in VT; NDVIb, Normalized Difference Vegetation Index in VT; NRIa, Nitrogen Reflectance Index in V8; StDEV; standard deviation. The 'node' is the main classification which represents the entire sample and may get split further into other nodes. 'Terminal node' is the mean of the observations in that node. 'Total count' is the number of observations in each terminal node.

stage was of equal importance to NRI in LPC detection. It is suggested by previous research that NDVI and NRI were viable N status indicators for a first N application when the canopy is not yet closed (Argento *et al.*, 2021), but in this experiment, they were also recognized as the best VIs at the end of the silage maize growing season. The superiority of the importance of these two VIs over other ones can be because some VIs have the great potential for suppressing soil noise, and

https://doi.org/10.1017/S0014479722000308 Published online by Cambridge University Press

others are good at antisaturation for vegetation spectra (Xu *et al.*, 2021). Therefore, effectively selecting sensitive features from indices and models to assess N status should be considered (Osco *et al.*, 2020).

Conclusions

Results suggested that most of the VIs (NDVI, NRI, CI, and MTVI2) taken by UAV and SPAD greenness index were strongly correlated to LPC in both the V8 and the VT growth stages. NRI was the most appropriate index among VIs, and it can provide a reliable model for the prediction of LPC, under a strong polynomial regression model in both developmental stages. These findings are appropriate for rapidly assessing crop protein status through VIs and models extracted from aerial multispectral imaging. In addition, these findings can be used for developing guidelines for farmers to utilize remote and proximal sensing technologies along with chemical analyzing methods to reduce the time and cost of assessments and adopting optimized strategies for N fertilizer management and timely harvest of the silage maize in semiarid conditions of Iran.

Supplementary materials. For supplementary material for this article, please visit https://doi.org/10.1017/S0014479722000308

Acknowledgment. The authors would like to thank Agricultural Engineering Research Institute for providing technical equipment (UAV and multispectral camera). The authors are also thankful to Mr. Hajian (the owner of the experimental farm) and Mr. Hamidreza Ibrahimi (UAV Pilot) for their cooperation.

Financial support. None.

Conflict of interest. The authors declare no competing interests.

References

Argento F., Anken T., Abt F., Vogelsanger E., Walter A. and Liebisch F. (2021). Site-specific nitrogen management in winter wheat supported by low-altitude remote sensing and soil data. *Precision Agriculture* **22**(2), 364–386.
Bagheri, N. (2016). Development of a high-resolution aerial remote-sensing system for precision agriculture. *International Journal of Remote Sensing* **38** (8–10), 2053–2065.
Bagheri, N., Ahmadi, H., Alavipanah, S. K. and Omid, M. (2012). Soil-Line vegetation indices for corn nitrogen content prediction. *International Agrophysics* **26**, 103–108.
Bagheri, N., Ahmadi, H., Alavipanah, S. K., and Omid, M. (2013). Multispectral remote sensing for site-specific nitrogen fertilizer management. *Pesquisa Agropecuária Brasileira* **48**, 1394–1401.
Cao X., Sun H., Wang C., Ren X., Liu H. and Zhang Z. (2018). Effects of late-stage nitrogen fertilizer application on the starch structure and cooking quality of rice. *Journal of the Science of Food and Agriculture* **98**(6), 2332–2340.
Caturegli L., Corniglia M., Gaetani M., Grossi N., Magni S., Migliazzi M., Angelini L., Mazzoncini M., Silvestri N., Fontanelli M., Raffaelli M., Peruzzi A. and Volterrani M. (2016). Unmanned aerial vehicle to estimate nitrogen status of turfgrasses. *PloS One* **11**(6), e0158268.
Chen X., Dong Z., Liu J., Wang H., Zhang Y., Chen T., . . . Du Y., Shao L. and Xie J. (2020). Hyperspectral characteristics and quantitative analysis of leaf chlorophyll by reflectance spectroscopy based on a genetic algorithm in combination with partial least squares regression. *Spectrochimica Acta Part A: Molecular and Biomolecular Spectroscopy* **243**, 118786.
Corti M., Cavalli D., Cabassi G., Vigoni A., Degano L. and Gallina P.M. (2019). Application of a low-cost camera on a UAV to estimate maize nitrogen-related variables. *Precision Agriculture* **20**(4), 675–696.
Darby H.M. and Lauer J.G. (2002). Harvest date and hybrid influence on corn forage yield, quality, and preservation. *Agronomy Journal* **94**(3), 559–566.
Devadas R., Lamb D.W., Simpfendorfer S. and Backhouse D. (2009). Evaluating ten spectral vegetation indices for identifying rust infection in individual wheat leaves. *Precision Agriculture* **10**(6), 459–470.
Diker K. and Bausch W.C. (2003). Potential use of nitrogen reflectance index to estimate plant parameters and yield of maize. *Biosystems Engineering* **85**(4), 437–447.
Galieni A., D'Ascenzo N., Stagnari F., Pagnani G., Xie Q. and Pisante M. (2020). Past and future of plant stress detection: an overview from remote sensing to Positron Emission Tomography. *Frontiers in Plant Science* **11**, 1975.

Gitelson A.A., Chivkunova O.B. and Merzlyak M.N. (2009). Nondestructive estimation of anthocyanins and chlorophylls in anthocyanic leaves. *American Journal of Botany* **96**(10), 1861–1868.

Gous P.W., Warren F., Mo O.W., Gilbert R.G. and Fox G.P. (2015). The effects of variable nitrogen application on barley starch structure under drought stress. *Journal of the Institute of Brewing* **121**(4), 502–509.

Guebel D.V., Nudel B.C. and Giulietti A.M. (1991). A simple and rapid micro-Kjeldahl method for total nitrogen analysis. *Biotechnology Techniques* **5**(6), 427–430.

Haboudane D., Miller J.R., Pattey E., Zarco-Tejada P.J. and Strachan I.B. (2004). Hyperspectral vegetation indices and novel algorithms for predicting green LAI of crop canopies: Modeling and validation in the context of precision agriculture. *Remote Sensing of Environment* **90**(3), 337–352.

Hatfield J.L., Gitelson A.A., Schepers J.S. and Walthall C.L. (2008). Application of spectral remote sensing for agronomic decisions. *Agronomy Journal* **100**(3), 117–131.

Jaberi-Aghdam M., Momayezi M.R., Bagheri N., Azizi P. and Nasri M. (2020). Detection of excess nitrogen stress of corn and hazards with aerial multi-spectral imaging by UAV. *Environmental Management Hazards* **7**(2), 163–180. (In Persian with English abstract).

Klopfenstein T.J., Erickson G.E. and Berger L.L. (2013). Maize is a critically important source of food, feed, energy and forage in the USA. *Field Crops Research* **153**, 5–11.

Li-Hong X.U.E., Wei-Xing C.A.O. and Lin-Zhang Y.A.N.G. (2007). Predicting grain yield and protein content in winter wheat at different N supply levels using canopy reflectance spectra. *Pedosphere* **17**(5), 646–653.

Lin F.F., Deng J.S., Shi Y.Y., Chen L.S. and Wang K. (2010). Investigation of SPAD meter-based indices for estimating rice nitrogen status. *Computers and Electronics in Agriculture* **71**, S60–S65.

López-Calderón M.J., Estrada-Ávalos J., Rodríguez-Moreno V.M., Mauricio-Ruvalcaba J.E., Martínez-Sifuentes A.R., Delgado-Ramírez G. and Miguel-Valle E. (2020). Estimation of total Nitrogen content in forage maize (Zea mays L.) using spectral indices: Analysis by random forest. *Agriculture* **10**(10), 451.

Mandić V., Bijelić Z., Krnjaja V., Simić A., Petričević M., Mićić N. and Caro-Petrović V. (2018). Effect of harvesting time on forage yield and quality of maize. *Biotechnology in Animal Husbandry* **34**(3), 345–353.

Nasielski J., Earl H. and Deen B. (2019). Luxury vegetative nitrogen uptake in maize buffers grain yield under post-silking water and nitrogen stress: A mechanistic understanding. *Frontiers in Plant Science* **10**, 318.

Nguy-Robertson A.L. (2013). The mathematical identity of two vegetation indices: MCARI2 and MTVI2. *International Journal of Remote Sensing* **34**(21), 7504–7507.

Osco L.P., Junior J.M., Ramos A.P.M., Furuya D.E.G., Santana D.C., Teodoro L.P.R. and Teodoro P.E. (2020). Leaf nitrogen concentration and plant height prediction for maize using UAV-based multispectral imagery and machine learning techniques. *Remote Sensing* **12**(19), 3237.

Padilla F.M., de Souza R., Peña-Fleitas M.T., Gallardo M., Gimenez C. and Thompson R.B. (2018b). Different responses of various chlorophyll meters to increasing nitrogen supply in sweet pepper. *Frontiers in Plant Science* **9**, 1752.

Padilla F.M., Gallardo M., Peña-Fleitas M.T., De Souza R. and Thompson R.B. (2018a). Proximal optical sensors for nitrogen management of vegetable crops: A review. *Sensors* **18**(7), 2083.

Pettersson C.G. and Eckersten H. (2007). Prediction of grain protein in spring malting barley grown in northern Europe. *European Journal of Agronomy* **27**(2–4), 205–214.

Pettersson C.G., Söderström M. and Eckersten H. (2006). Canopy reflectance, thermal stress, and apparent soil electrical conductivity as predictors of within-field variability in grain yield and grain protein of malting barley. *Precision Agriculture* **7**(5), 343–359.

Rahimi Jahangirlou M., Akbari G.A., Alahdadi I., Soufizadeh S., Kumar U. and Parsons D. (2021b). Phenotypic traits, grain yield and yield components of Maize cultivars under combinations of management practices in semi-arid conditions of Iran. *International Journal of Plant Production* **15**(3), 459–471.

Rahimi Jahangirlou M., Akbari G.A., Alahdadi I., Soufizadeh S., Ludemann C. and Parsons D. (2022). Phenotypic predictors of dent maize grain quality based on different genetics and management practices. *Journal of Cereal Science,* 103388.

Rahimi Jahangirlou M., Akbari G.A., Alahdadi I., Soufizadeh S. and Parsons D. (2021a). Grain quality of maize cultivars as a function of planting dates, irrigation and Nitrogen stress: A case study from semiarid conditions of Iran. *Agriculture* **11**(1), 11.

Reum D. and Zhang Q. (2007). Wavelet based multi-spectral image analysis of maize leaf chlorophyll content. *Computers and Electronics in Agriculture* **56**(1), 60–71.

Shendryk Y., Sofonia J., Garrard R., Rist Y., Skocaj D. and Thorburn P. (2020). Fine-scale prediction of biomass and leaf nitrogen content in sugarcane using UAV LiDAR and multispectral imaging. *International Journal of Applied Earth Observation and Geoinformation* **92**, 102177.

Smith A.M., Bourgeois G., Teillet P.M., Freemantle J. and Nadeau C. (2008). A comparison of NDVI and MTVI2 for estimating LAI using CHRIS imagery: A case study in wheat. *Canadian Journal of Remote Sensing* **34**(6), 539–548.

Wang L.W. and Wei Y.X. (2013). Progress in inversion of vegetation nitrogen concentration by hyperspectral remote sensing. *Spectroscopy and Spectral Analysis* **33**(10), 2823–2827.

Xiong D., Chen J., Yu T., Gao W., Ling X., Li Y., . . . Huang J. (2015). SPAD-based leaf nitrogen estimation is impacted by environmental factors and crop leaf characteristics. *Scientific Reports* **5**(1), 1–12.

Xu X., Fan L., Li Z., Meng Y., Feng H., Yang H. and Xu B. (2021). Estimating leaf Nitrogen content in corn based on information fusion of multiple-sensor imagery from UAV. *Remote Sensing* **13**(3), 340.

Zhao H., Song X., Yang G., Li Z., Zhang D. and Feng H. (2019). Monitoring of nitrogen and grain protein content in winter wheat based on Sentinel-2A data. *Remote Sensing* **11**(14), 1724.

Cite this article: Bagheri N, Rahimi Jahangirlou M, and Jaberi Aghdam M. Predicting protein content of silage maize using remotely sensed multispectral imagery and proximal leaf sensing. *Experimental Agriculture*. https://doi.org/10.1017/S0014479722000308